J. Meas. Sci. Instrum., 2024, 15(1): 64-71.
DOI: 10.62756/jmsi.1674-8042.2024007
http://jmsi.publish.founderss.cn/
jmsi@nuc.edu.cn

Maximum photovoltaic power point tracking based on hybrid GWO-P&O algorithm under local shadow

ZHAO Feng, XIAO Chengrui*, CHEN Xiaoqiang, WANG Ying
School of Automation and Electrical Engineering, Lanzhou Jiaotong University, Lanzhou 730070, China

***Corresponding author:** XIAO Chengrui (3206906420@qq.com)

Received: February 5, 2023 **Revised:** April 18, 2023 **Accepted:** April 28, 2023

Abstract: In view of the problem of multiple peak values of P-U characteristic curve under a local shading environment, the traditional gray wolf optimization (GWO) is slow in convergence speed and low in accuracy of steady state at the late stage when tracking the maximum power point. Combining the advantages of GWO and perturbation & observation (P&O) method, an improved hybrid maximum power point tracking (MPPT) algorithm based on GWO-P&O was proposed. Firstly, optimized by the GWO, the algorithm was gradually close to the global MPPT. Then, P&O was introduced into the GWO at the late convergence stage, so that the local maximum power point of of photovoltaic power can be found at a faster speed while maintaining a high steady-state accuracy of the GWO, which overcomes the shortcomings of the traditional GWO algorithm. Finally, the proposed method was compared with the GWO under different environments. The results show that the proposed GWO-P&O method can improve the convergence speed in the late stage of the GWO when tracking the maximum power while ensuring high steady-state accuracy.

Key words: gray wolf optimization (GWO); perturbation & observation (P&O) method; partial shading environment; hybrid maximum power point tracking (MPPT) algorithm; global maximum power point

0 Introduction

With the support of the national strategy of "Achieving carbon neutrality by 2060", how to reduce the consumption of fossil energy by improving the efficiency of clean energy has been an important research topic[1]. As a kind of high-quality green energy, solar energy has attracted much attention owing to its simplicity to install for power generation equipment and low cost of maintenance[2,3]. To capture more light energy and reduce light rejection, it is necessary to eliminate the influence of environmental factors such as local shading caused by dust particles in the air and changes of clouds in the movement trajectory in the sky, which may affect the output power of photovoltaic array and thus reduce the power generation efficiency[4-6]. At present, the maximum power point tracking (MPPT) technology focuses on solving the problem of low conversion efficiency of photovoltaic array due to environmental changes[7], especially in a harsh environment.

In a uniform lighting environment, traditional MPPT algorithms such as perturbation & observation (P&O) [8] and incremental conductance (INC) [9] can accurately track the maximum power point of photovoltaic power. Whereas in practical engineering, the external environment constantly changes. When the light radiation of photovoltaic arrays are uneven, especially for local shadow caused by various weather effects, the traditional MPPT control strategy is difficult to track the real maximum power point and easy to fall into local extremum, affecting the output power of entire photovoltaic power system. In response to this problem, various advanced intelligent control algorithms have been successively applied to it. For example, Dileep et al.[10] applied particle swarm optimization (PSO) to the maximum power control of photovoltaic power system, which corrects the defect that the global maximum power point could not be traced due to the unreasonable setting of inertia weight ω. The results show that under the action of the adaptive inertia weight factor, the improved PSO can deal with the influence of various environmental changes well. However, related parameters need to be set, resulting in being cumbersome to use. Sheng et al.[11] realized MPPT based on artificial bee colony algorithm. The algorithm is combined with differential evolution algorithm to effectively shorten the tracking time, reduce the steady-state error and speed the convergence. However, it is prone to discard the global power extreme points during tracking, and its stability needs to be further improved. There have been enhanced leader PSO (EL-PSO) [12], fuzzy-PSO[13], gray wolf optimization with fuzzy logic controller (GWO-FLC) [14] and other composite algorithms[15-17] for tracking the maximum power point, which can effectively cope with the dynamic change of the environment, save search time and reduce power oscillation loss. Meanwhile the make up for the disadvantages of the traditional single algorithm. Rakumar et al. [18] proposed a maximum power tracking control algorithm based on GWO to solve the problems of steady-state oscillation, slow global convergence and low tracking accuracy under partially sheltered environmental conditions. Compared with traditional P&O and intelligent control algorithms based on PSO, the MPPT system based on GWO algorithm has higher steady-state accuracy and efficiency under local shading, however, it takes a long time to search the maximum power point in the later stage, which increases the power loss.

Considering outstanding global optimization ability of GWO and fast convergence speed of P&O method, we proposed a hybrid GWO-P&O algorithm for the maximum photovolatic power point tracking in case of local shadow to improve tracking speed and accuracy.

1 Mathematical model of photovoltaic array under partial shading

1.1 Mathematical model of photovoltaic cell

The equivalent circuit of a single-diode photovoltaic cell is shown in Fig.1.

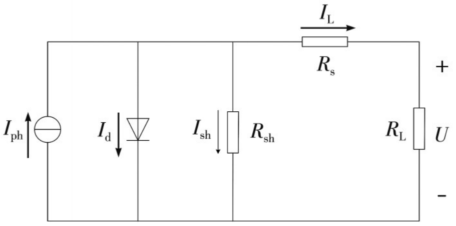

Fig. 1 Equivalent circuit of a single-diode photovoltaic cell

The current through the equivalent diode of the photovoltaic cells can be got by

$$I_d = I_o\left[\exp\left(\frac{q(U+I_L R_s)}{AKT}\right)-1\right]. \tag{1}$$

According to Kirchhoff's current law, the relationship between output voltage U and current I_L of the equivalent model of photovoltaic cell with single diode can be obtained as[19]

$$I_L = I_{ph} - I_o\left[\exp\left(\frac{q(U+I_L R_s)}{AKT}\right)-1\right] - \frac{U+I_L R_s}{R_{sh}}. \tag{2}$$

The mathematical model used in actual engineering is shown as

$$C_1 = \left(1-\frac{I_{mp}}{I_{sc}}\right)\exp\left(\frac{-U_{mp}}{C_2 U_{oc}}\right), \tag{3}$$

$$C_2 = \left(\frac{U_{mp}}{U_{oc}}-1\right)\left[\ln\left(1-\frac{I_{mp}}{I_{sc}}\right)\right], \tag{4}$$

$$I_L = I_{sc}\left\{1 - C_1\left[\exp\left(\frac{U}{C_2 U_{oc}}\right)-1\right]\right\}, \tag{5}$$

where I_o is the reverse saturation current (A); I_{ph} is photogenerated current (A); I_L is the output current (A); U is the output voltage (V); R_s and R_{sh} are the series and parallel resistors of the equivalent model of single diode, respectively (Ω); A is the quality factor of PN junction, which generally ranges from 1.00 to 1.25; K is Boltzmann constant (1.38×10^{-23} J·K^{-1}); T is the temperature of photovoltaic cell (℃); q is the charge of the electron (1.602×10^{-19} C); C_1 and C_2 are correction coefficients; I_{mp} is the output current corresponding to the maximum power point of photovoltaic cell (A); U_{mp} is the output voltage (V) corresponding to the maximum power point of the photovoltaic cell; I_{sc} is the short-circuit current (A); and U_{oc} is the open circuit voltage (V).

1.2 Multi-peak mathematical model of photovoltaic array

The structure of photovoltaic array is shown in Fig.2.

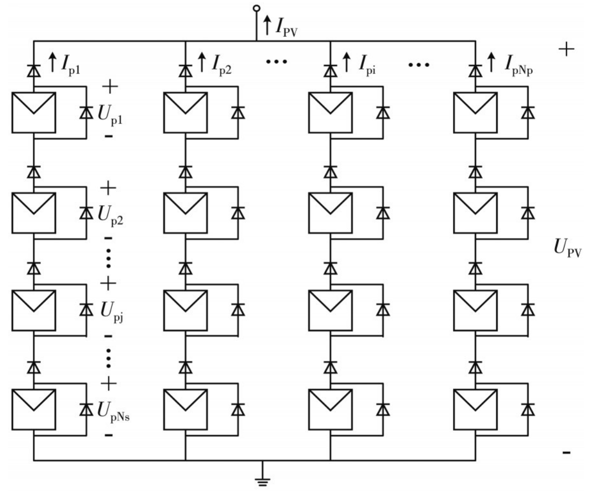

Fig. 2 Structure of PV array

In practice, to improve the output power of photovoltaic array, photovoltaic module is often composed of photovoltaic cells in series, and photovoltaic array is composed of photovoltaic modules in parallel. When the photovoltaic array is in the local shading environment, the photovoltaic cells in the photovoltaic array will produce local temperature rise, forming the “hot spot effect”. Therefore, parallel diodes are often used to avoid this phenomenon, as shown in Fig.2[20].

The multi-peak mathematical model of photovoltaic array under shading is expressed as[21]

$$I_{\mathrm{PV}}=\sum_{i=1}^{N_{\mathrm{p}}} I_{\mathrm{p}i}=N_{\mathrm{p}}\left(I_{\mathrm{ph}}-I_{\mathrm{d}}-\frac{U_{\mathrm{p}j}+I_{\mathrm{p}i} R_{\mathrm{s}}}{R_{\mathrm{sh}}}\right), \tag{6}$$

$$U_{\mathrm{PV}}=\sum_{j=1}^{N_{\mathrm{s}}} U_{\mathrm{p}j}, \tag{7}$$

where I_{PV} is the output current of the entire photovoltaic array(A); U_{PV} is the output voltage of the whole photovoltaic array(V) ; $I_{\mathrm{p}i}$ is the output current of photovoltaic module (A); $U_{\mathrm{p}j}$ is the output voltage of the photovoltaic module(V); N_{p} is the number of parallel connections of photovoltaic modules and N_{s} is the number of series of photovoltaic cells.

2 MPPT control method based on GWO-P&O

2.1 GWO

GWO mainly simulates the habits of collective hunting of wolves to find the optimal solution. The principle of cooperative predation is shown in Fig.3.

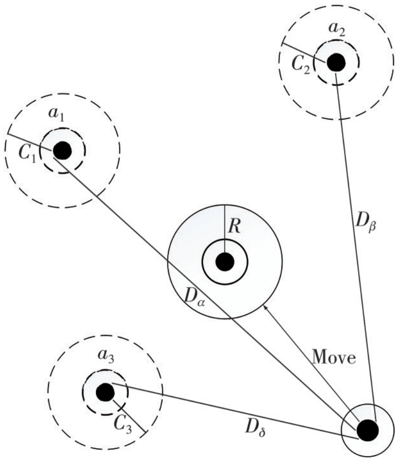

Fig. 3 Principles of cooperative predation by gray wolves

Since GWO can adjust convergence factor automatically, and it is simpler and more convenient in practical application, it can accurately track the global extreme point and reduce the steady-state error in the maximum power tracking of photovoltaic array in a changeable environment.

Fig.4 shows the division of the social hierarchy within the gray wolf population. There are ω, δ, β and α from bottom to top, and the ability of the gray wolf individuals within the population is gradually weakened. ω is at the bottom of the social hierarchy, which is responsible for coordinating and handling the balance of relationships within wolves, and α is the decision maker of various affairs in the group and has the highest power. The predation strategy of gray wolf consists of encircling, attacking and searching the target prey.

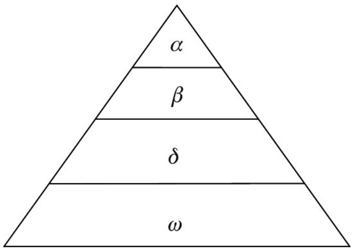

Fig. 4 Social hierarchy of gray wolf population

2.1.1 Surrounding target prey

In the encircled process, gray wolves constantly update their positions by identifying the position of target prey, so as to carry out the encircled strategy: the current position of gray wolves closest to the target prey is regarded as the optimal solution, then other gray wolves dynamically update their positions to approach the optimal position, and finally the prey is surrounded by gray wolves. The process of gray wolves rounding up prey is defined as[22]

$$D=\left|C X_{\mathrm{P}}(t)-X(t)\right|, \tag{8}$$

$$X(t+1)=X_{\mathrm{P}}(t)-A D, \tag{9}$$

where D is the distance between the prey and the gray wolf; $X_{\mathrm{P}}(t)$ is the position of the current prey at iteration t; t is the current iteration number; $X(t+1)$ is the position updating formula of gray wolf; and A and C are the synergy coefficients.

The calculation formula of A and C are shown as

$$A=2 a r_1-a, \tag{10}$$

$$C=2 r_2, \tag{11}$$

where a is the convergence factor, and its value decreases linearly from 2 to 0 with the increase of iterations; and r_1 and r_2 are random numbers within $[0,1]$.

2.1.2 Attacking target prey

When gray wolves determine the location of the prey, other gray wolves (including ω) dynamically update their positions according to the optimal location of gray wolves. β and δ will lead the wolves to surround the prey under the guidance of α, realizing the purpose of approaching the prey. The process of searching target prey is defined as

$$\begin{cases} D_\alpha=\left|C_1 X_\alpha-X\right|, \\ D_\beta=\left|C_2 X_\beta-X\right|, \\ D_\delta=\left|C_3 X_\delta-X\right|, \end{cases} \tag{12}$$

where X_α, X_β and X_δ are the current positions of α, β and δ, respectively; D_α, D_β and D_δ are the distances between α, β and δ and other gray wolves, respectively; C_1, C_2 and C_3 are random vectors; and X is the current position of other gray wolf individuals.

The step length, direction and final position of gradually approaching α, β and δ are defined as

$$\begin{cases} X_1 = X_\alpha - A_1 D_\alpha, \\ X_2 = X_\beta - A_2 D_\beta, \\ X_3 = X_\delta - A_3 D_\delta, \end{cases} \tag{13}$$

$$X(t+1) = \frac{X_1 + X_2 + X_3}{3}, \tag{14}$$

where A_1, A_2 and A_3 are coefficients related to A, and their values change within $[-a, a]$ as a decreases.

2.1.3 Searching for target prey

Each gray wolf searches for prey independently by locating α, β and δ before gathering together to attack the prey. As shown in Fig.5, when $|A|>1$, wolf individuals will separate from prey (local optimal solution) to find a more suitable prey (the global optimal solution); When $|A|<1$, the optimal position of wolf individual will be chosen and updated to carry out local searching.

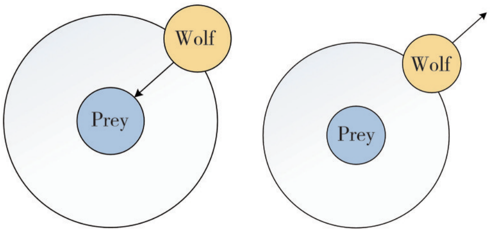

(a) $|A|<1$ (b) $|A|>1$

Fig. 5 Schematic of hunting for target prey

2.1.4 Principle of GWO applied to MPPT

The specific steps flow of GWO are as follows.

1) Initialization of gray wolf population, a, A_1, A_2, A_3 and C_1, C_2, C_3.

2) The fitness of gray wolves is calculated and top 3 wolves of the best fitness are reserved, including α, β and δ.

3) Update of the current position of gray wolf.

4) Update of a, A_1, A_2, A_3 and C_1, C_2, C_3.

5) The fitness of all gray wolves is calculated.

6) Update of the fitness and locations of α, β and δ.

7) Judging whether end condition is met. If not, return to Step 3.

In our work, when GWO was applied to MPPT of photovoltaic array, taking the real-time power of photovoltaic array as fitness function, the position of gray wolf corresponded to duty cycle. According to the principle of GWO, the location of gray wolves was constantly updated by searching, encircling and hunting, so that gray wolves can gather in the direction of the optimal solution and finally prey.

2.2 P&O algorithm

P&O algorithm is the most widely used MPPT method because of its simplicity and ease of implementation. The purpose of P&O algorithm applied to the MPPT of photovoltaic array is to judge the direction of power change by sampling voltage and current of photovoltaic array. Its principle is shown in Fig.6.

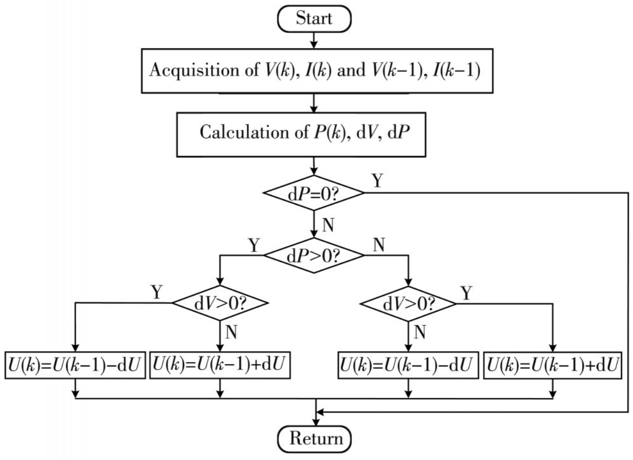

Fig. 6 Flow chart of P&O algorithm

2.3 Hybrid MPPT method based on GWO-P&O

Although GWO needs to adjust fewer parameters when applied to MPPT, it also has the following shortcomings[23].

1) The convergence rate is slow in the later stage. Gray wolves mainly determine the distance between themself and the prey by judging the locations of α, β and δ, which is related to the search mechanism of GWO.

2) It is prone to falling into the local optimal solution. In the iterative process, ω keeps approaching the first three wolves, but it is not guaranteed that α is the global optimal power point.

In view of the above problems, we combined GWO with P&O for MPPT of photovoltaic array. The global search performance of GWO was used to quickly converge to the maximum power point. Then P&O method was introduced in the late convergence stage, thus improving the tracking speed and steady-state characteristics. Furthermore, it is necessary to set termination decision strategy for GWO when GWO was executed. Here, if the number of iterations is greater than 5, GWO will be converted to P&O algorithm. As a result, the proposed MPPT algorithm will stabilize near the maximum power point at a faster speed and reduce the power fluctuation.

The flow chart of MPPT algorithm based on GWO-P&O is shown in Fig.7.

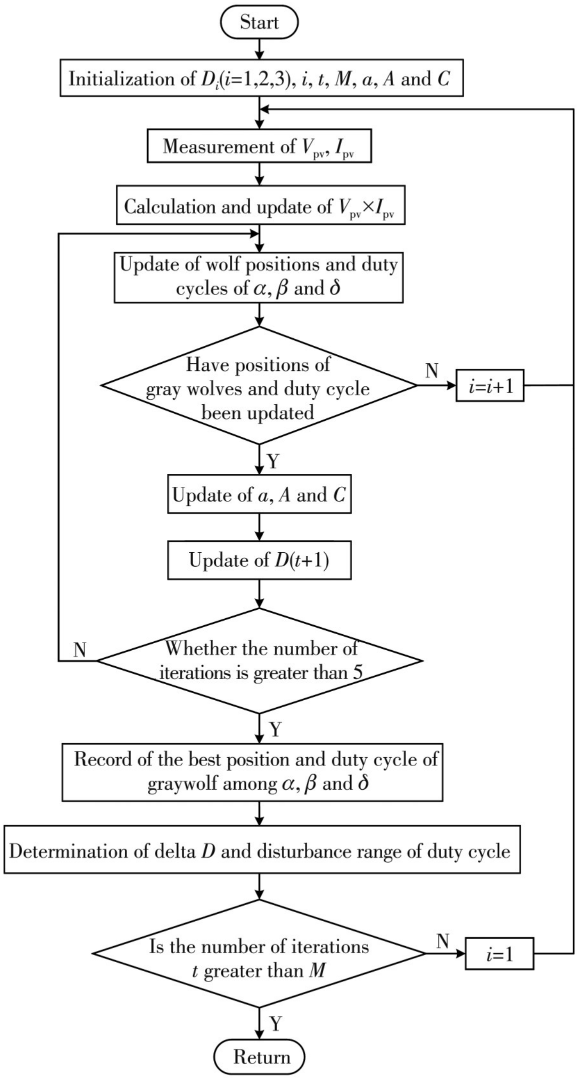

Fig. 7 Flow chart of MPPT algorithm based on GWO-P&O

3 Results and discussion

3.1 Parameter settings

To verify the effectiveness of the proposed MPPT algorithm based on GWO-P&O, we used Matlab/Simulink simulation software to build a 5×1 simulation model of photovoltaic array. The specific parameters are listed in Table 1.

Table 1 Specific parameters of photovoltaic arrays

Parameters	Values
Open-circuit voltage U_{oc}/V	36.3
Short-circuit current I_{sc}/A	7.84
Maximum output voltage U_{mp}/V	29
Maximum output current I_{mp}/A	7.35

The block diagram of MPPT of photovoltaic array is shown in Fig.8, which consists of photovoltaic array, a Boost converter, a load and measurement control unit. The output voltage and current of photovoltaic array are firstly collected and measured by the MPPT controller. The voltage of the operating point of photovoltaic array is controlled for MPPT by adjusting the duty cycle.

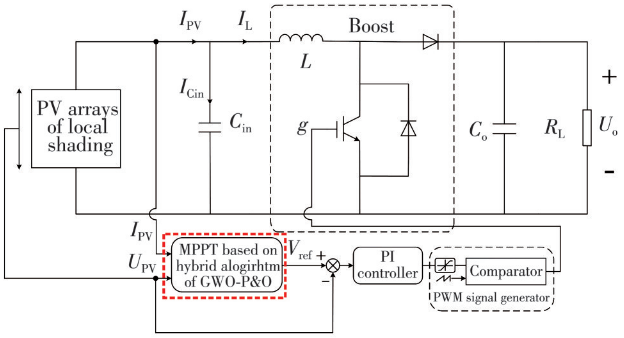

Fig. 8 Boost-based MPPT of photovoltaic array

To analyze the effect of MPPT algorithm, the index of steady-state error is given as

$$e=\frac{P_{\mathrm{MPP}}-P_{\mathrm{out}}}{P_{\mathrm{MPP}}}\times 100\%. \tag{15}$$

3.2 Results and discussion

3.2.1 MPPT under uniform illumination

When the photovoltaic array is under uniform illumination, the P-U output produces a single peak curve, as shown in Fig. 9. If the radiation intensity of the photovoltaic array is set to be 1 000 W·m^{-2}, the maximum power of the photovoltaic array is 8.52 kW and the corresponding voltage is 290 V.

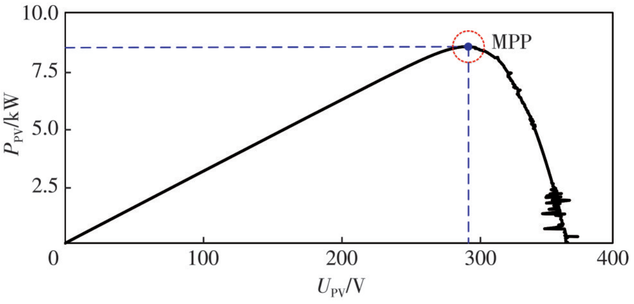

Fig. 9 P-U output characteristic curve under uniform illumination

The simulation time was set to be 1 s, the MPPT algorithm based on GWO-P&O were compared with that based on GWO. Fig.10(a), (b) and (c) show the comparison results of output power, voltage and current of photovoltaic array based on GWO and GWO-P&O algorithm, respectively, and Fig. 10(d) shows the comparison results of the voltages of DC bus.

As can be seen from Fig.10, under uniform illumination, MPPT system based on GWO tracks to the maximum power point after 0.75 s, with a maximum power point of approximate 8.510 kW and a steady-state error of 0.171%. However, the MPPT system based on GWO-P&O

converges to the maximum power point after 0.25 s, with a maximum power of 8.519 kW and an error of only 0.01%. The results indicate that the MPPT based on GWO-P&O has faster tracking speed and higher steady-state accuracy.

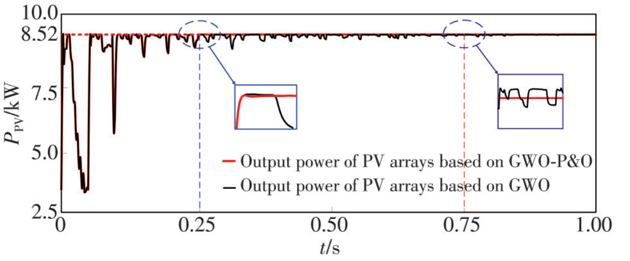

(a) Comparison of output powers of photovoltaic array

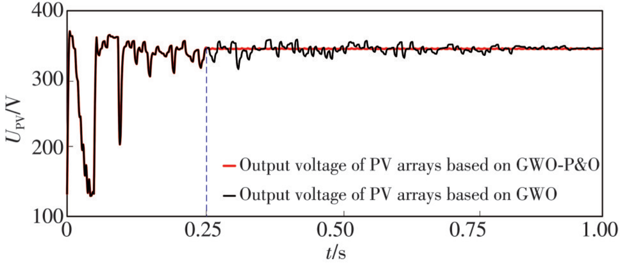

(b) Comparison of output voltages of photovoltaic array

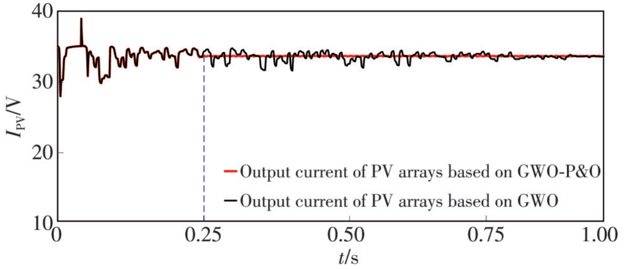

(c) Comparison of output currents of photovoltaic array

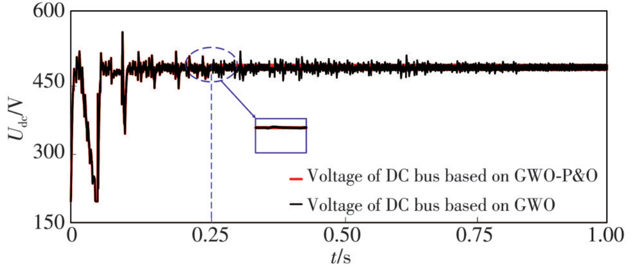

(d) Comparison of voltages of DC bus

Fig. 10 Comparison of GWO-P&O and GWO under uniform illumination

3.2.2 MPPT under local shading

When local shielding occurs, the irradiance of the photovoltaic array will become uneven. The *P*-*U* output produces a multi-peak curve, as shown in Fig.11. When *v* the irradiance values of the photovoltaic array are set to be 1 000 W·m^{-2}, 1 000 W·m^{-2}, 400 W·m^{-2} and 800 W·m^{-2}, respectively, the maximum output power of the photovoltaic array is 5.76 kW and the corresponding voltage is 240.2 V.

The simulation time was set to be 1 s, the MPPT algorithm based on GWO-P&O were compared with GWO. Fig.12 (a), (b) and (c) show the comparison results of output power, voltage and current of photovoltaic array based on GWO and GWO-P&O, respectively, and Fig. 12(d) shows the comparison results of the voltages of DC bus.

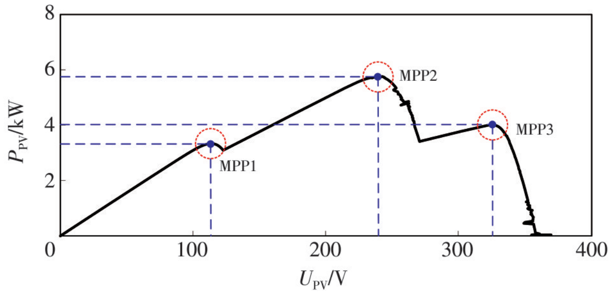

Fig. 11 *P*-*U* output characteristic curve under local shading

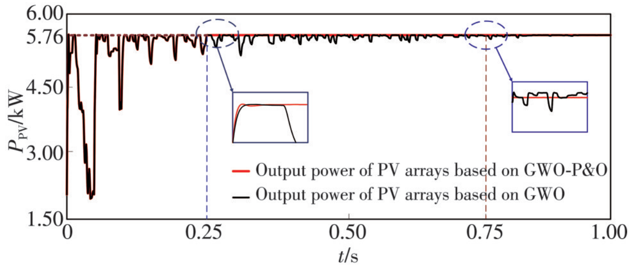

(a) Comparison of output powers of photovoltaic array

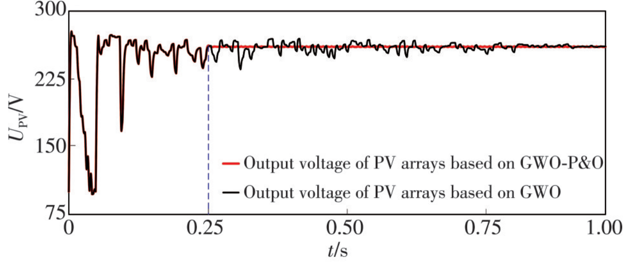

(b) Comparison of output voltages of photovoltaic array

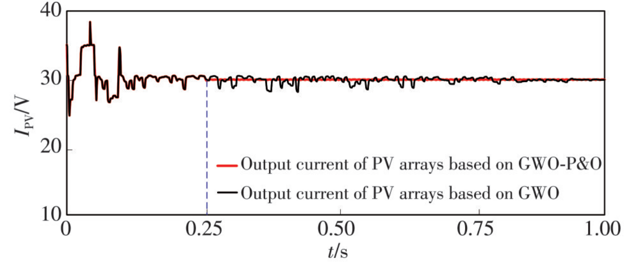

(c) Comparison of output currents of photovoltaic array

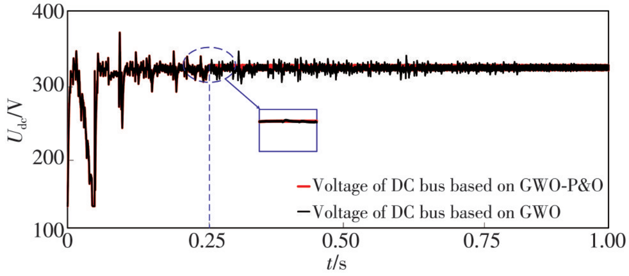

(d) Comparison of voltages of DC bus

Fig. 12 Comparison of GWO-P&O and GWO under local shading

As can be seen from Fig. 12, in the case of local shading, MPPT system based on GWO tracks to the maximum power point after 0.75 s, with a maximum power point of approximate 5.748 kW and a steady-state error of 0.208%. However, the MPPT system based on GWO-P&O converges to the maximum power point after 0.25 s, with a maximum power of 5.759 kW and an error of only 0.01%. The results indicate that the MPPT based on GWO-P&O has faster tracking speed and higher steady-state accuracy.

To sum up, the comparison results of the two MPPT algorithms under two environmental conditions are shown in Table 2.

Table 2 Comparison of simulation results under two environmental conditions

MPPT algorithm	Tracking time/s		Steady-state error/%	
	Under uniform illumination	Under local shadow	Under uniform illumination	Under local shadow
GWO	0.75	0.75	**0.171**	**0.208**
GWO-P&O	0.25	0.25	0.010	0.010

As can be seen from Table 2, compared with MPPT method based on GWO, the MPPT method based on GWO-P&O has obvious advantages in tracking speed and steady-state accuracy under two environmental conditions.

4 Conclusions

In a local shading environment, the *P-U* output of photovoltaic array produces a multi-peak curve, which makes it difficult for the traditional MPPT control method to accurate and quick global MPPT, thus affecting the utilization rate of photovoltaic array. Therefore, we proposed a hybrid control algorithm based on GWO-P&O, which can quickly and accurately track the MPP by virtue of the excellent global search performance of GWO and local search ability of P&O method. The conclusions are as follows.

1) Under uniform illumination, the proposed GWO-P&O has the outstanding advantages in tracking speed and steady-state error than GWO.

2) Compared with the traditional GWO, the proposed GWO-P&O has significantly faster tracking speed and higher accuracy in the case of local shading.

3) The proposed GWO-P&O can solve the problems of slow convergence speed and low steady-state accuracy of traditional GWO when tracking the MPP in the late period under the conditions of uniform illumination and local shading.

Acknowledgement

This work was supported by National Natural Science Foundation of China (No. 52067013); Natural Science Foundation of Gansu Province (No.21JR7RA280)

Declaration of conflicting interests

The authors have no conflict of interests related to this publication.

References

[1] YUAN Q, ZHAO B, WANG L, et al. Photovoltaic mutipeak MPPT control based on TSA-P&O hybrid algorithm. Journal of Power Systems and Automation, 2021, 33(12): 1-9.

[2] OHAMMADREZA A, KAZEM P. A novel reconfiguration procedure to extract maximum power from partially-shaded photovoltaic arrays. Solar Energy, 2018, 173: 110-119.

[3] XI J Z, LI F, ZHANG X, et al. Rt-lab simulation analysis of annual generating capacity of photovoltaic cell based on centralized loss. Automation of Electric Power Systems, 2018, 42(8): 156-162.

[4] BOSCO M J, MABEL M C. A novel cross diagonal view configuration of a PV system under partial shading conditions. Solar Energy, 2017, 158: 760-773.

[5] BANA S, SAINI R P. Experimental investigation on power output of different photovoltaic array configurations under uniform and partial shading scenarios. Energy, 2017, 1127: 438-453.

[6] DALIENTO S, DINAPOLI F, GUERRIERO P, et al. A modified bypass circuit for improved hot spot reliability of solar panels subject to partial shading. Solar Energy, 2016, 134: 211-218.

[7] XIE X H, LAI J J. Review of global maximum power point tracking control methods for photovoltaic arrays in local shadow. Power Grid Technology, 2014, 38(12): 3279-3285.

[8] MOHANTY S, SUBUDHI B, RAY P K. A grey wolf-assisted perturb & observe MPPT algorithm for a PV system. IEEE Transactions on Energy Conversion, 2017, 32(1): 340-347.

[9] KEY K S, MEKHILEF S. Modified incremental conductance MPPT algorithm to mitigate inaccurate responses under fast-changing solar irradiation level. Solar Energy, 2014, 133: 333-342.

[10] DILEEP G, SINGH S N. An improved particle swarm optimization based maximum power point tracking aigorithm for PV system operating under partial shading conditions. Solar Energy, 2017, 158: 1006-1015.

[11] SHENG S Q, CHEN Y L, ZHANG J J. Study on PV maximum power tracking strategy based on the differential evolution artificial swarm algorithm. Protection and Control

of Electric Power System, 2018, 46(11): 23-29.

[12] GAVHANE P S, KRISHNAMURTHY S, DIXIT R, et al. EL-PSO based MPPT for solar PV under partial shaded condition. Energy Procedia, 2017, 117: 1047-1053.

[13] ELDAHABA Y E A, SAAD N H, ZEKRY A. Enhancing the tracking techniques for the global maximum power point under partial shading conditions. Renewable and Sustainable Energy Reviews, 2017, 73: 1173-1183.

[14] ELTAMALY A M, FARH H M H. Dynamic global maximum power point tracking of the PV systems under variant partial shading using hybrid GWO-FLC. Solar Energy, 2019, 177: 306-316.

[15] SOUFI Y, BECHOUAT M, KAHLA S. Fuzzy-PSO controller design for maximum power point tracking in photovoltaic system. International Journal of Hydrogen Energy, 2017, 42: 8680-8688.

[16] LI G Q, JIN Y, AKRAM M W, et al. Application of bio-inspired algorithms in maximum power point tracking for PV systems under partial shading conditionsa-A review. Renewable and Sustainable Energy Reviews, 2017, 42: 8680-8688.

[17] GAO Z Q, LI S, ZHOU X S, et al. Application of linear autoperturbation in PV power generation system MPPT. Protection and Control of electric Power System, 2018, 46(15): 52-59.

[18] RAJKUMAR M V, MAHAKUMAR M, MANOJKUMA R M, et al. A new DC-DC converter topology with grey wolf MPPT algorithm for photovoltaic syste. International Journal of Emerging Technology & Research, 2017, 5(4): 54-59.

[19] WU D, XU C Y, ZHENG L J, et al. Research on the maximum power point tracking algorithm of photovoltaic system based on β parameters. Solar Journal, 2020, 41(6): 234-241.

[20] LI S Y, ZHANG W B, ZHAO X Z, et al. Improved whale algorithm optimized to support vector regression for photovoltaic maximum power point tracking. Electrotechnical Journal, 2021, 36(9): 1771-1781.

[21] LI Z J, ZHANG Y N, WANG L J, et al. Multimodal MPPT study based on improved quantum particle group algorithm. Solar Journal, 2021, 42(5): 221-229.

[22] ZHANG Q J, WANG K L, FANG X Q. Multipeak MPPT of photovoltaic array based on GWO algorithm. Journal of Jilin University (Natural Science Edition), 2018, 56(6): 1526-1532.

[23] ZHAO S Q, XIAO H, LIU Z B, et al. Maximum power point tracking of PV under partial shading based on CSA-IP&O. Protection and Control of Power System, 2020, 48(5): 26-32.

局部阴影下基于GWO-P&O混合算法的光伏最大功率点跟踪

赵 峰，肖成锐*，陈小强，王 英

兰州交通大学 自动化与电气工程学院，甘肃 兰州 730070

摘 要： 针对局部遮阴环境下传统灰狼优化(Gray wolf optimization，GWO)算法在跟踪最大功率点时P-U特性曲线出现多峰值、后期收敛速度慢、稳态精度低等问题，结合灰狼优化算法和扰动观察法(Perturbation and observation，P&O)各自的优势，提出了基于GWO-P&O的混合优化最大功率点跟踪(Maximum power point tracking，MPPT)算法。首先，采用灰狼优化算法逐渐向光伏的全局最大功率点靠近。其次，在灰狼优化算法收敛后期引入P&O法，既保持了灰狼优化算法较高的稳态精度，又能以较快速度寻找到局部最大功率点。最后，在不同环境工况下，将所提出的GWO-P&O方法与传统GWO算法进行对比。结果表明，改进的GWO-P&O算法在保证良好稳态性能的同时，一定程度上提高了GWO算法后期跟踪最大功率时的收敛速度。

关键词： 灰狼优化算法；扰动观察法；局部遮阴；混合优化最大功率点跟踪算法；全局最大功率点

引用格式： ZHAO Feng, XIAO Chengrui, CHEN Xiaoqiang, et al. Maximum photovoltaic power point tracking based on hybrid GWO-P&O algorithm under local shadow. Journal of Measurement Science and Instrumentation, 2024, 15(1): 64-71.